J|A|C|S
ARTICLES
Published on Web 03/30/2006

The Structure of Liquid Tetrahydrofuran

Daniel T. Bowron,*[,†,‡] John L. Finney,[‡] and Alan K. Soper[†,‡]

Contribution from the ISIS Facility, CCLRC Rutherford Appleton Laboratory, Chilton, Didcot, Oxon OX11 0QX, U.K., and Department of Physics and Astronomy, University College London, Gower Street, London WC1E 6BT, U.K.

Received December 7, 2005; E-mail: D.T.Bowron@rl.ac.uk

Abstract: Hydrogen/deuterium isotopic substitution neutron diffraction techniques have been used to measure the structural correlation functions of liquid tetrahydrofuran at room temperature. Empirical potential structure refinement (EPSR) has been used to build a three-dimensional model of the liquid structure that is consistent with the experimental data. Analysis to the level of the orientational correlation functions shows that the liquid displays a preference for T-like configurations between the tetrahydrofuran molecules, a local structure that results in voidlike regions of approximately 1.25 Å radius within the bulk liquid. The surface chemistry of these voids suggests a slightly positive electrostatic character. These findings are consistent with the known propensity of the liquid to solvate free electrons.

1. Introduction

The remarkable combination of physicochemical properties of the small cyclic ether, tetrahydrofuran, has led to its frequent adoption as a favored solvent medium. It exhibits high volatility, a low freezing point, and the ability to solvate both polar and nonpolar compounds. In consequence tetrahydrofuran has found application in areas as diverse as the production of polymer coatings and adhesives to pharmaceutical chemistry where it provides a clean solvent that can be readily separated from desired products. It is also stable in strongly basic solution conditions, and thus, its utility extends to the support of complex catalytic chemistry and Grignard reagents.[1]

The use of tetrahydrofuran as a novel solvent has recently been extended into the area of solvated electron investigations that are of importance in improving our understanding of electron-transfer reactions and radiation chemistry.[2,3] The cyclic ether was selected as an ideal nonpolar medium as it does not spontaneously produce solvated electrons on solvation of alkali metal atoms such as sodium.[2] As a nonpolar liquid without strong dipolar forces, in comparison to more polar solvent analogues, tetrahydrofuran is thought to allow the creation of larger volumes in which free electrons can be accommodated.[3] Recent computational studies further suggest that the electronic structure of the solvated electron in a weakly polar liquid will be controlled by the solvent structure itself.[4]

When considering the importance and extensive use of this solvent, it is perhaps surprising that the current understanding of its fundamental liquid structure is almost exclusively derived from computer simulation studies.[5−10] All these investigations have been parametrized to reproduce reasonably macroscopic physical properties such as the liquid's diffusion coefficient or specific heat capacity, but they are entirely dependent upon the resulting interatomic and intermolecular force fields for the reproduction of structural parameters. Due to this absence of any parametrization to data directly related to atomic and molecular structure, conclusions derived from the models concerning molecular interactions and local structure remain largely speculative.

Over the past decade, significant advances have been made in the methods of neutron diffraction with isotopic substitution[11] and in the development of more powerful computational tools for inverting the resulting experimental data to three-dimensional structural models.[12] Consequently, it is now feasible to experimentally establish the structure of this important solvent. Here we present the results of a neutron diffraction investigation of the structure of liquid tetrahydrofuran at room temperature. The use of hydrogen−deuterium isotopic substitution to enhance the contrast in the experimental scattering patterns confers enhanced reliability on the intermolecular structural information that can be extracted from the resulting model.

2. Experimental Section

The neutron scattering data were collected using the small angle neutron diffractometer for amorphous and liquid samples (SANDALS) at the ISIS pulsed neutron and muon source at the Rutherford Appleton Laboratory, Oxfordshire, UK. This instrument is optimized for the study

[†] ISIS Facility, CCLRC Rutherford Appleton Laboratory.
[‡] Department of Physics and Astronomy, University College London.

(1) Lyondell Chemical Company, Application Data Sheet 2608-V4-1004 2004.
(2) Barthel, E. R.; Martini, I. B.; Schwartz, B. J. *J. Chem. Phys.* **2000**, *112*, 9433.
(3) Martini, I. B.; Barthel, E. R.; Schwartz, B. J. *J. Chem. Phys.* **2000**, *113*, 11245.
(4) Bedard-Hearn, M. J.; Larsen, R. E.; Schwartz, B. J. *J. Chem. Phys.* **2005**, *122*, 134506.
(5) Chandrasekhar, J.; Jorgensen, W. L. *J. Chem. Phys.* **1982**, *77*, 5073.
(6) Chandrasekhar, J.; Jorgensen, W. L. *J. Chem. Phys.* **1982**, *77*, 5080.
(7) Bedard-Hearn, M. J.; Larsen, R. E.; Schwartz, B. J. *J. Phys. Chem. B* **2003**, *107*, 14464.
(8) Girard, S.; Muller-Plathe, F. *Mol. Phys.* **2003**, *101*, 779.
(9) Bedard-Hearn, M. J.; Larsen, R. E.; Schwartz, B. J. *J. Chem. Phys.* **2005**, *122*, 134506.
(10) Rayon, V. M.; Sordo, J. A. *J. Chem. Phys.* **2005**, *122*, 204303.
(11) Finney, J. L.; Soper, A. K. *Chem. Soc. Rev.* **1994**, *23*, 1.
(12) McGreevy, R. L. *J. Phys. Condens. Matter* **2001**, *13*, R877.

of light element-containing liquids and glasses and in particular for hydrogen/deuterium isotopic substitution techniques.

To facilitate the direct extraction of the intermolecular structural correlations between tetrahydrofuran molecules, three samples were measured: (1) C_4H_8O, (2) C_4D_8O, and (3) a 1:1 mixture of C_4H_8O and C_4D_8O. Each sample was contained in a flat plate cell of internal dimensions 1 mm × 35 mm × 35 mm constructed from $Ti_{0.68}Zr_{0.32}$ alloy with a wall thickness of 1.1 mm for each surface bounding the internal volume. The alloy composition was chosen such that the cell would not produce any coherent neutron scattering contribution to the measured signal. This simplifies the data analysis as the "null-scattering" cell makes no structural contribution to the data that would complicate the analysis of the molecular system. During measurement the cell was maintained at the ambient temperature of the instrument ~25 °C.

The scattering data were collected over scattering angles (2θ) between 3° and 40° and analyzed using neutron wavelengths in the range $\lambda = 0.075-3.5$ Å over a corresponding Q-range for each data set ranging from 0.1 to 30 $Å^{-1}$. After collection the data were analyzed using the Gudrun routines[13] that are based upon basic algorithms in the widely used ATLAS package.[14] These routines correct the data for the contributions from the empty cell, instrument background, absorption, and multiple scattering and normalize the data to absolute units using the scattering of a vanadium standard. The remaining corrections to account for the contributions from inelastic scattering by the sample were made using the methods outlined in Soper and Luzar.[15]

3. Theory

Following corrections, the function extracted from a neutron diffraction measurement is the total structure factor $F(Q)$, also known as the interference differential cross section, which is defined in terms of the magnitude of the scattering vector, Q.

$$Q = \frac{4\pi}{\lambda}\sin\theta \tag{1}$$

Here λ is the wavelength of the incident neutrons, and 2θ is the scattering angle. The total structure factor can then be written as:

$$F(Q) = \sum_{\alpha\leq\beta}(2-\delta_{\alpha\beta})c_\alpha c_\beta b_\alpha b_\beta (S_{\alpha\beta}(Q)-1) \tag{2}$$

The structure factor contains information relating to the pairwise spatial correlations between atoms of type α and β, reflected in the sum over the partial structure factors, $S_{\alpha\beta}(Q)$. These terms are weighted by the respective concentrations, c_α and c_β, and scattering lengths, b_α and b_β, of each atom type. To avoid double counting of the like terms within the summation, $\delta_{\alpha\beta}$ is the Kronecker delta function.

The structure factors, either composite or partial, can be inverted to real space atomic pair distribution functions, $g_{\alpha\beta}(r)$, by a Fourier transform weighted by the atomic density, ρ:

$$(S_{\alpha\beta}(Q)-1) = 4\pi\rho\int_0^\infty r^2\,(g_{\alpha\beta}(r)-1)\frac{\sin Qr}{Qr}\mathrm{d}r \tag{3}$$

$g_{\alpha\beta}(r)$ represents the real space correlations between pairs of atoms as a function of their separation, r, and is the primary aim of most structural studies of liquids and disordered materials. In addition to the interatomic distance information, integrating this function over a range in r allows us to access the number of atoms of type β that would be found around an atom of type α within the specified range, or vice versa.

To access directly the partial pair distribution functions by neutron scattering techniques, it is necessary to perform a series of diffraction measurements. In each measurement the contrast of the total structure factor is varied by changing the isotopic composition of the sample. In each of the measured total structure factors the relative contributions that come from the pair interaction terms involving the substituted atomic sites is different. As the fractional composition and scattering lengths of each sample are known, the result is a set of simultaneous equations in $S_{\alpha\beta}(Q)$. These can be solved for the partial structure factors involving the isotopically varied atomic species.[11] The method assumes that under the prevailing pressure and temperature conditions of the measurement, the structure of the system of interest is isotope invariant, and also that isotopes with distinctly different neutron scattering properties are available for each of the required atom types. For complex systems with more than two atom types, it is generally not possible, or practical, to perform enough isotope variation experiments to extract all the partial structure factors required to completely characterize the system. The experimental data are thus, more often than not, incomplete with regards to a total solution. Fortunately, modern computational techniques allow us to address successfully this incompleteness problem.

What is required is a three-dimensional model of the structure of the disordered system that is consistent with the available experimental data. Classical computational techniques such as Monte Carlo simulation have now evolved to the point where obtaining this is a realistic possibility. The underlying premise is that the more experimental data used to constrain the model, the more reliable the final model. Once such a molecular level model exists, we can access any site−site partial distribution function of interest as well as evaluate the most likely molecular orientational correlation functions. We are thus now able to access detailed molecular level structural information for a range of liquids and solutions.[16−19]

4. Data Modeling

In this study the technique of empirical potential structure refinement[20,21] has been used to build a three-dimensional model of the structure of liquid tetrahydrofuran that is consistent with the three measured total structure factors measured for C_4H_8O, C_4D_8O, and the 1:1 mixture. As there is no in-solution isotopic exchange of hydrogens between the various molecular sites, the isotopic variation experiments intrinsically weight the model toward the intermolecular correlations. The modeling process additionally combines this information with a basic knowledge of the structure of the molecule and the atomic density of the system to refine the structure of the liquid. In this respect, the refinement procedure used has strong similarities with certain structure refinement techniques used in refining macromolecular crystal structures.[22]

(13) Soper, A. K. Private Communication, 2005.
(14) Soper, A. K.; Howells, W. S.; Hannon, A. C. *ATLAS − Analysis of Time-of-Flight Diffraction Data from Liquid and Amorphous Samples*; Rutherford Appleton Laboratory Report, RAL 89-046, 1989.
(15) Soper, A. K.; Luzar, A. *J. Chem. Phys.* **1992**, *97*, 1320.
(16) Bowron, D. T.; Finney, J. L.; Soper, A. K. *J. Phys. Chem. B* **1998**, *102*, 3551.
(17) Soper, A. K. *Mol. Phys.* **2001**, *99*, 1503.
(18) Hardacre, C.; Holbrey, J. D.; McMath, S. E. J.; Bowron, D. T.; Soper, A. K. *J. Chem. Phys.* **2003**, *118*, 273.
(19) Thompson, H.; Wasse, J. C.; Skipper, N. T.; Howard, C. A.; Bowron, D. T.; Soper, A. K. *J. Phys. Condens. Matter* **2004**, *16*, 5639.
(20) Soper, A. K. *Chem. Phys.* **1996**, *202*, 298.
(21) Soper, A. K. *Phys. Rev. B.* **2005**, *72*, 104204.

Table 1. Lennard-Jones, Charge and Atomic Mass Parameters Used for the Reference Potentials that Seed the Empirical Potential Structure Refinement Model of Liquid Tetrahydrofuran

atom type	ϵ kJ mole^{-1}	σ Å	*M* amu	*q* e
O	0.586	2.90	16	−0.400
C1	1.251	3.21	12	0.140
C2	1.251	3.21	12	0.000
M1	0.791	2.58	2	0.030
M2	0.791	2.58	2	0.000

The following labels were assigned to the atomic sites on the tetrahydrofuran molecule: O for the oxygen within the five-membered ring, C1 for the carbon atoms that are connected to the oxygen atom, C2 for the carbon atoms only connected to other carbon atoms, and M1 and M2 for the hydrogen atoms bonded to C1 and C2 carbon atoms, respectively. The Lennard-Jones parameters, atomic masses, and fractional charges used to seed the modeling process are summarized in Table 1, while Table 2 summarizes the interatomic distance constraints used to define the basic molecular geometry of the tetrahydrofuran molecule.

The structure refinement was initialized using an equilibriated Monte Carlo simulation of 216 tetrahydrofuran molecules in a cubic box of side length 30.8 Å at 298 K, corresponding to an atomic density of 0.096 atoms Å^{-3}. Cubic periodic boundary conditions were used. As the aim of the refinement procedure was to reproduce experimental data, the simulated molecules are allowed to adopt a range of configurations within a harmonic potential approximation. The atoms within the molecule are distributed by specifying a harmonic potential between pairs of atoms centered on their mean separation. They are redistributed according to the same potential at regular intervals throughout the simulation. During whole molecule moves and rotations, however, they remain fixed within the molecular coordinate system. This procedure is necessary to account for the intrinsic Debye−Waller-type variation in the measured structural data. The mean intramolecular bond lengths and atomic distances were constrained to the values given in Table 2.

An iterative procedure is used to drive the simulated structure toward agreement with the experimental data. This is achieved through the application of perturbations to the intermolecular site−site potentials. These perturbations are derived iteratively from the difference between the measured diffraction data and the corresponding functions calculated from the evolving simulation.[21] Once the structural model and associated perturbation potentials reach satisfactory agreement with the experimental data, the simulation is allowed to proceed without further perturbation of the potential functions and ensemble average structural information accumulated for interrogation. As outlined by Soper,[21] the empirical potential extracted by this method is expressed as a sum Poisson distributions as a function of site−site separation, and there is one term for each pair of atom types in the simulation. The simulation is Monte Carlo, run in the NVT ensemble, so that dynamic and other thermodynamic information, apart from the configurational energy and pressure, is not directly available from the EPSR simulation itself. However, it is possible that the same potentials could be incorporated into an MD simulation of the same system, thus giving dynamic information, provided however that the molecular geometries from the EPSR simulation are retained. A general rule of thumb is that the amplitude of the empirical potential is only a fraction, typically about 10%, of the reference potential which it is perturbing, although this may be different in particular cases.

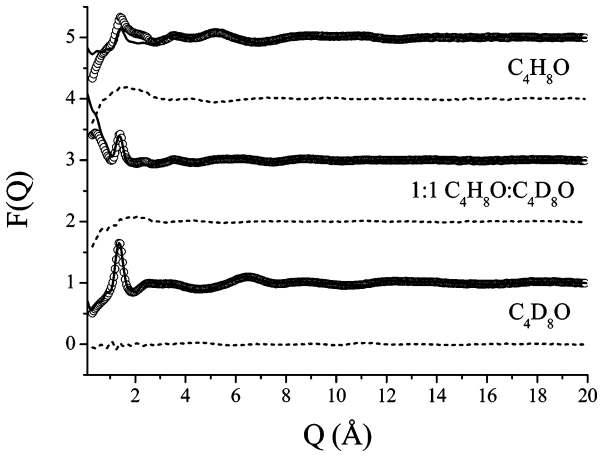

Figure 1. Experimentally measured total structure factor data (open circles) and EPSR refined fits (solid lines) for neutron scattering data collected on C_4D_8O, a 1:1 mixture of C_4H_8O and C_4D_8O, and C_4H_8O. The fit residuals (broken lines) for C_4D_8O, the mixture, and for C_4H_8O are shown vertically offset around $F(Q) = 0$, 2 and 4, respectively.

5. Results

Figure 1 shows the experimental data and EPSR-refined model fits and residuals obtained for the three independent interference differential cross section data sets. The overall quality of the fits is seen to be good although a low frequency residual is found in the fits to the mixture and the protiated sample. In real space, this residual component would correspond to unphysically short-range interatomic correlations. It is attributed to imperfect correction of the inelastic scattering contribution from light hydrogen in the neutron scattering signal, and this is consistent with the observation that the magnitude of the fit residual is greatest for C_4H_8O and smallest for C_4D_8O.

Table 2. Intramolecular Distance Constraints Used To Define the Basic Structure of the THF Molecule

d/Å	O	$C1_1$	$C1_2$	$C2_1$	$C2_2$	$M1_{C11}$	$M1_{C11}$	$M1_{C12}$	$M1_{C12}$	$M2_{C21}$	$M2_{C21}$	$M2_{C22}$	$M2_{C22}$
O		1.42	1.42	2.33	2.37	2.06	2.08	2.08	2.05	3.29	2.70	2.88	3.28
$C1_1$			2.31	1.53	2.33	1.10	1.10	3.07	3.03	2.20	2.17	2.69	3.32
$C1_2$				2.36	1.53	2.82	3.22	1.10	1.10	3.34	2.72	2.17	2.20
$C2_1$					1.52	2.17	2.19	3.28	2.87	1.10	1.10	2.16	2.19
$C2_2$						2.69	3.32	2.19	2.17	2.20	2.16	1.10	1.10
$M1_{C11}$							1.80	3.27	3.76	2.45	3.08	2.58	3.76
$M1_{C11}$								4.03	3.74	2.69	2.46	3.76	4.21
$M1_{C12}$									1.80	4.15	3.79	2.37	2.78
$M1_{C12}$										3.92	2.81	3.05	2.38
$M2_{C21}$											1.82	2.43	2.71
$M2_{C21}$												3.06	2.45
$M2_{C22}$													1.81
$M2_{C22}$													

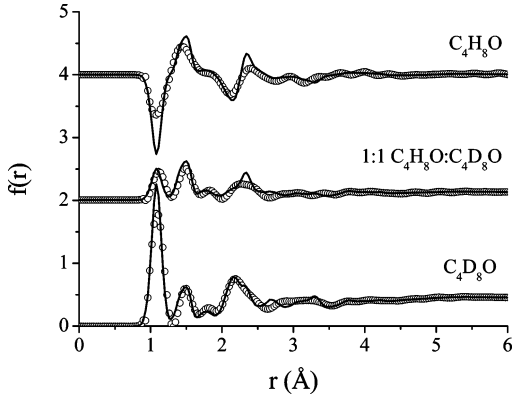

Figure 2. Composite radial distribution function data determined by direct Fourier transform of the experimental data (open circles) and EPSR refined fits (solid lines) for neutron scattering data collected on C_4D_8O, a 1:1 mixture of C_4H_8O and C_4D_8O and C_4H_8O.

Figure 2 shows the total distribution functions, $f(r)$, that are obtained by direct Fourier transform of the experimental structure factor data and the corresponding functions calculated from the EPSR refined model. Although the distribution functions determined by direct Fourier transform of the experimental data are likely to be subject to considerable termination effects and are thus unsuitable for detailed intermolecular structure determination, they do allow the underlying quality of the basic intramolecular model to be evaluated. The overestimation in the simulation of the peak heights at ∼1 Å and ∼2.4 Å indicates that, although the model of the tetrahydrofuran molecule explores a range of configurations, the intramolecular C−H bonds and cross-ring correlations are slightly overconstrained as the results indicate insufficient broadening of structural contributions that contribute in these specific distance ranges. Despite this, when judged across the whole distance range dominated by the intramolecular correlations, the general model appears reasonable. In this context, we note that earlier simulation studies[5] investigating the impact of the intramolecular structure on the intermolecular interactions suggest that slight imperfections in this area will not unduly affect the intermolecular structure determined from the liquid model.

The intermolecular site−site partial distribution functions for tetrahydrofuran are shown in Figures 3 and 4. These figures illustrate the correlations between the atom types on the

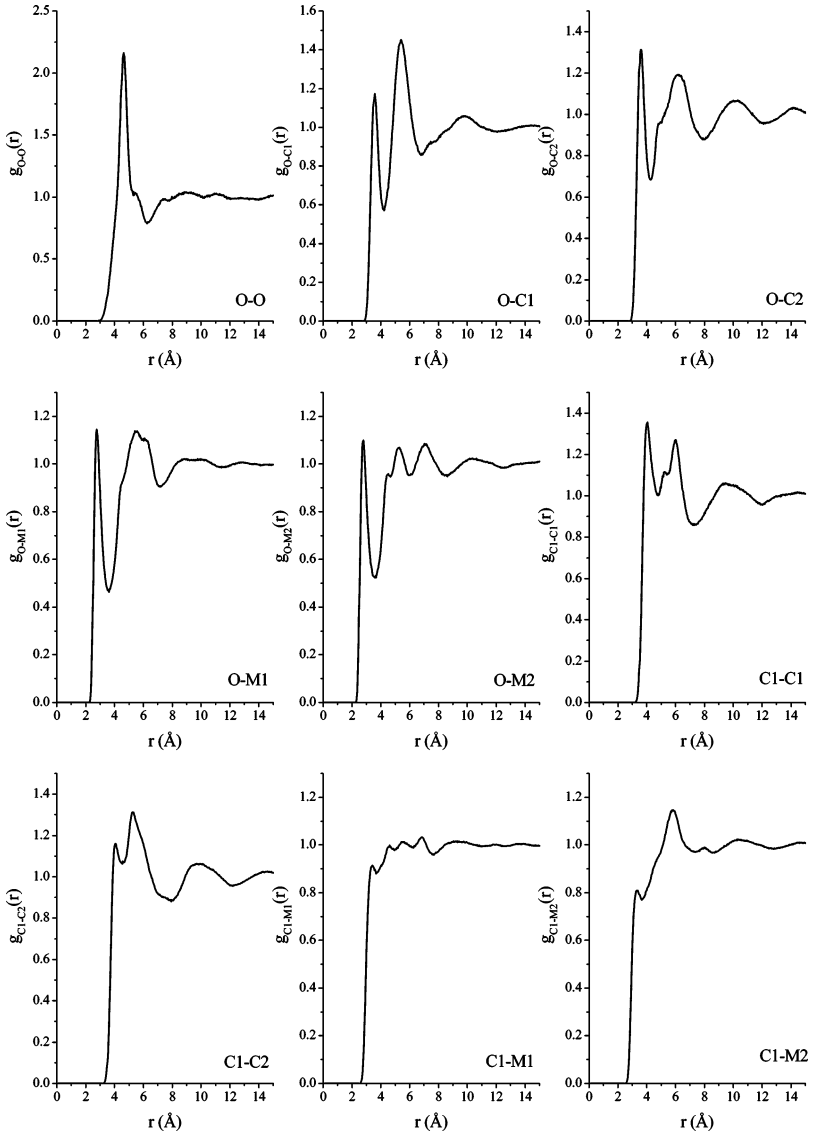

Figure 3. Intermolecular partial distribution functions derived by the EPSR procedure (1): O−O, O−C1, O−C2, O−M1, O−M2, C1−C1, C1−C2, C1−M1, C1−M2, for pure tetrahydrofuran at room temperature.

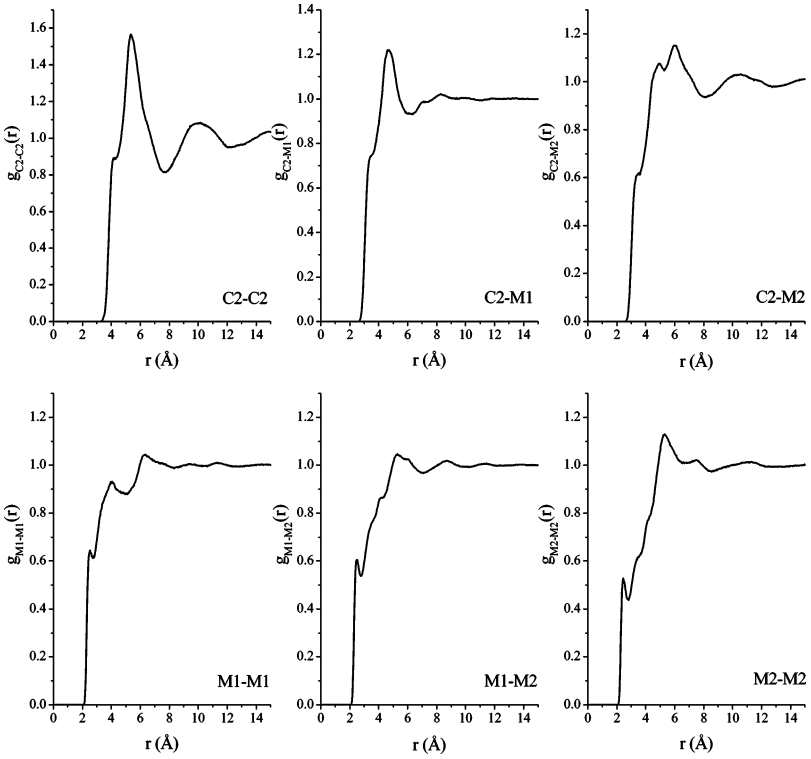

Figure 4. Intermolecular partial distribution functions derived by the EPSR procedure (2): C2−C2, C2−M1, C2−M2, M1−M1, M1−M2, M2−M2 for pure tetrahydrofuran at room temperature.

Table 3. Coordination Numbers Obtained by Integration of the Features in the Indicated Partial Distrubution Functions

correlation	atomic density (atom Å^{-3})	R_{min} (Å)	R_{max} (Å)	coordination number (atoms)
O−O	0.0073	3.0	5.3	4.1 ± 0.2
		3.0	6.3	7.0 ± 0.3
O−C1	0.0147	2.9	4.2	2.2 ± 0.1
		4.2	6.8	15.8 ± 0.3
C1−O	0.0073	2.9	4.2	1.1 ± 0.1
		4.2	6.8	7.9 ± 0.1
O−C2	0.0147	2.9	4.2	2.5 ± 0.1
		4.2	7.9	26.2 ± 0.3
C2−O	0.0073	2.9	4.2	1.2 ± 0.1
		4.2	7.9	13.0 ± 0.2
O−M1	0.0295	2.3	3.6	2.9 ± 0.1
		3.6	7.1	37.9 ± 0.4
M1−O	0.0073	2.3	3.6	0.7 ± 0.1
		3.6	7.1	9.4 ± 0.1
O−M2	0.0295	2.3	3.6	2.9 ± 0.1
M2−O	0.0073	2.3	3.6	0.7 ± 0.1
C2−C2	0.0147	3.4	4.4	1.6 ± 0.1
		4.4	7.7	24.9 ± 0.3
THF−THF	0.0073	3.7	7.6	12.6 ± 0.3

distinguishable units that make up the cyclic molecule: O, C1, C2, M1, and M2. Table 3 provides the coordination numbers calculated by integrating under the indicated features in the pair distribution functions. Figure 5 shows the molecular centers correlation function; this is defined as the radial distribution of the molecular geometric centers calculated using the oxygen and carbon atoms of the cyclic ether. Integrating under this first peak of the centers function shows that, on average, each tetrahydrofuran molecule has 12.6 ± 0.3 neighboring molecules in the distance range from 3.7 to 7.6 Å (Table 3). This experimental result immediately provides us with a means to discriminate between the various potential models suggested in the literature[8] where results have been found with both single-

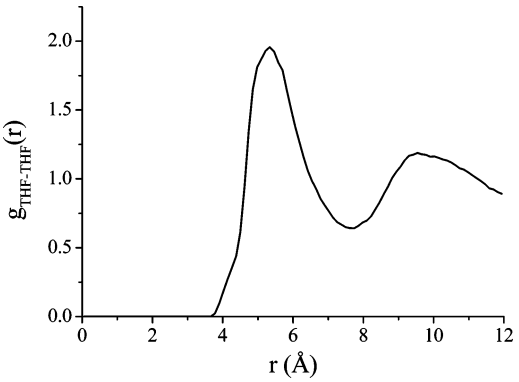

Figure 5. EPSR-derived molecular centers distribution function for liquid tetrahydrofuran at room temperature. The center of the molecule is defined as the geometric center of the oxygen atom and four carbon atoms that make up the five-membered ring.

and double-peak structures in the intermolecular interaction range from 4 to 8 Å. The neutron scattering data clearly support those potentials resulting in single-peak structures.

6. Orientational Correlation Functions and the Three-Dimensional Structure of the Liquid

Though the partial distribution functions give us quantitative access to the pairwise interactions between the atoms that make up the molecules, we need to understand the liquid structure in terms of an average three-dimensional model. For a molecular system, and in particular for a cyclic molecule such as tetrahydrofuran with varying atomic character around its ring, a useful function is the orientational correlation function which effectively removes the angular averaging from the pair distribution functions. The simplest orientational function to interpret is the spatial density function (SDF),[23] in this case $g_{THF-THF}(r,\Omega)$, which represents a three-dimensional map of the

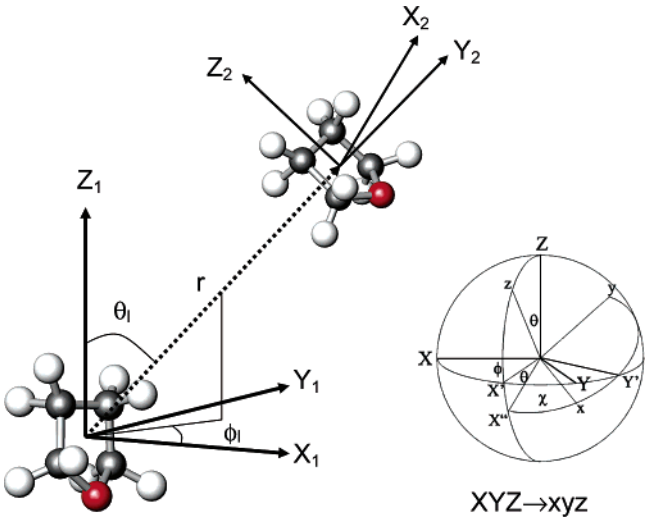

Figure 6. Coordinate axes reference frames of the tetrahydrofuran molecule used in the spherical harmonic representation of the relative molecular orientations. The inset coordinate axes illustrate the transformation scheme characterized by the Euler angle convention ($\phi\theta\chi$) used to go from the frame of reference *XYZ* to *xyz*. (Note that $Y'' = Y'$, $Z' = Z$, and $Z'' =$ z.)

density of neighboring molecule centers around an oriented central molecule as a function of radial distance, *r*, and angular position, $\Omega(=\theta,\phi)$, relative to the coordinate frame assigned to the central molecule.

Figure 6 shows the coordinate reference frame for the tetrahydrofuran molecules used in the orientational correlation analysis. Molecule 1, at the origin, defines the basic coordinate axes, and the location of neighboring molecule centers are defined using the variables (r,ϕ_1,θ_1). The origin of the molecule is defined by the geometric center of the five-membered ring, the *Z*-axis is defined from the origin to pass midway between the two C2 carbons of the molecule, the *X*-axis is defined to be perpendicular to the ring plane, and the *Y*-axis is defined to be orthogonal to *Z* and *X*. The relative orientation of molecule 2, at coordinates (r,ϕ_1,θ_1), is then specified in terms of the three Euler angles (ϕ_2,θ_2,χ_2) which govern the transformation for the coordinate reference axes from position (*X*,*Y*,*Z*) to (*x*,*y*,*z*) in the standard fashion:[24] (1) rotate about the *Z*-xis positively by ϕ ($0° \le \phi \le 360°$), (2) rotate positively about Y' by θ ($0° \le \theta \le 180°$), and finally, (3) rotate positively about Z'' by χ ($0° \le \chi \le 360°$), where the positive direction is defined to be that by which a right-handed screw would advance.

Figure 7 shows the spatial density function calculated to show the regions of space around a tetrahydrofuran molecule that are most likely to be occupied by the molecular centers of a neighboring molecule in the liquid. The isosurface shown has been chosen to enclose the most probable regions in the radial distance range from 3.5 to 7.0 Å at the 30% occupancy level. Three regions of space are highlighted. First, there is a dominant region in the SDF defined by a large lobe positioned below the oxygen atom of the oriented central tetrahydrofuran molecule that extends upward and outward to encompass the region along the *x*-axis of the central molecule. Second there are two lobes to either side of the C2 carbons on the central molecule, and finally there is a small lobe oriented perpendicular to the plane of the central molecule above the two C2 carbons in the ring.

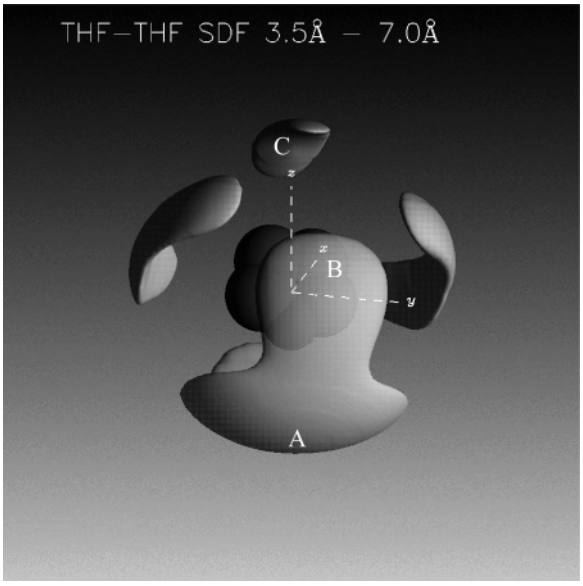

Figure 7. EPSR-derived spatial density function, $g_{THF-THF}(r,\Omega)$, showing the distribution of tetrahydrofuran molecular centers around a central tetrahydrofuran molecule as a function of distance, *r*, and orientation, $\Omega(=\theta,\phi)$. The isosurface is calculated to show the most probable regions of space that would be occupied by the top 30% of the neighboring molecules that make up the complete coordination shell in the distance range from 3.5 to 7 Å. The scale of the viewport window is ±10 Å. The labels (A), (B), and (C) identify the spatial regions where the orientational correlations of neighboring molecules have been calculated and displayed in Figure 8.

These three regions relate respectively to strongly polar, slightly polar, and nonpolar regions of the central molecule.

We can now look at the preferred orientation of neighboring water molecules associated with a selection of the spatial regions identified in Figure 7. The relevant orientational correlation maps are shown in Figure 8 with schematic ball-and-stick type diagrams to aid the reader shown in Figure 9. Panel (A) focuses on the preferred orientation of a neighboring tetrahydrofuran molecule that would be found in the distance range from 3.5 to 7.0 Å and immediately below the oxygen atom of the central molecule shown in Figure 7, $\theta_1 = 180°$. This is essentially at the apex of the lobe that relates to intermolecular interactions with the polar oxygen atom of a tetrahydrofuran molecule placed at the origin. The orientational correlation function appears as a wavelike continuous band circumscribing the coordinate system origin at the center of panel (A). This plot tells us that the molecular contacts in this approach geometry would be largely T-like with the oxygen atom of the central molecule pointing into the center of a neighboring tetrahydrofuran molecular ring as illustrated in Figure 9A. The continuous ring indicates that the neighboring molecule is free to rotate, while the wavelike form suggests the plane of this molecule slightly cants, depending upon the electrostatic interactions between the negatively charged oxygen on its ring with the slightly positively charged CH_2 groups of the central molecule.

Figure 8, Panel (B) shows the preferred orientation of a tetrahydrofuran molecule that would approach a central molecule in the direction perpendicular to the plane of the ring, along the *x*-axis of Figure 7, $\theta_1 = 90°$. The two symmetric lobes at

(22) Finney, J. L. *Struct. Chem.* **2002**, *13*, 231.
(23) Svishchev, I. M.; Kusalik, P. G. *J. Chem. Phys.* **1993**, *99*, 3049.
(24) Gray, C. G.; Gubbins, K. E. *Theory of Molecular Fluids, Volume 1: Fundamentals*; International Series of Monographs on Chemistry 9, Clarendon Press: Oxford, 1984.

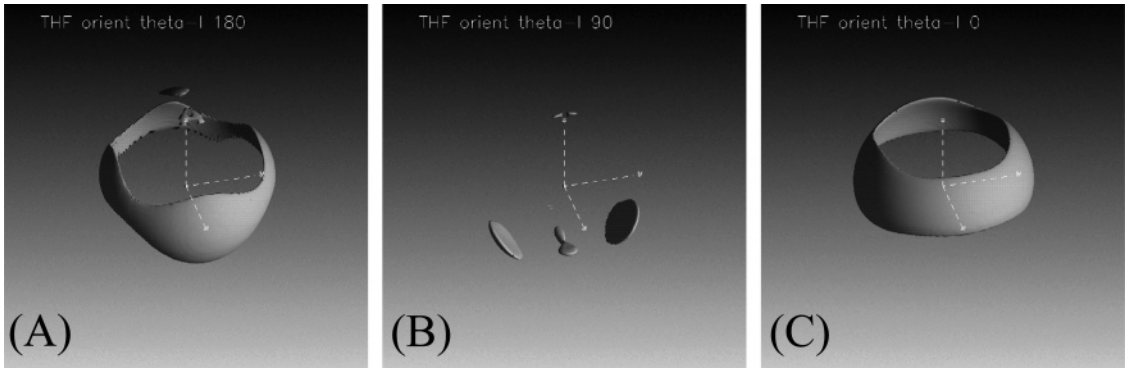

Figure 8. EPSR-derived orientational correlation maps as a function of (ϕ_2,θ_2) or (θ_2,χ_2) showing the preferred orientation of tetrahydrofuran molecules as a function of angular position (ϕ_1,θ_1) and distance (r), relative to a central tetrhydrofuran molecule. The isosurface is calculated to show the most probable orientations at the 30% level of tetrahydrofuran molecules in the first coordination shell distance range from 3.5 to 7 Å. (A) (ϕ_2,θ_2) preferred orientation map of a molecule found immediately below the oxygen atom of the central tetrahydrofuran molecule shown in Figure 6 ($\theta_1 = 180°$, $\phi_1 = 0°$, $\chi_2 = 0°$). (B) (θ_2,χ_2) preferred orientation map corresponding to favored regions for a tetrahydrofuran molecule approaching perpendicular to the plane of the central molecule along the x-axis of Figure 6, ($\theta_1 = 90°$, $\phi_1 = 0°$, $\phi_2 = 0°$), and finally, (C) (ϕ_2,θ_2) preferred orientation map of a tetrahydrofuran molecule that would be found in the nonpolar lobe highlighted above the C2 carbons shown in Figure 6 ($\theta_1 = 0°$, $\phi_1 = 0°$, $\chi_2 = 0°$). The scale of the viewport window is ±10Å.

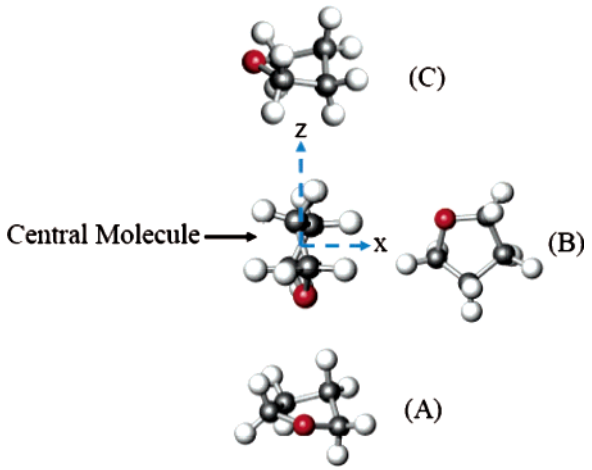

Figure 9. Schematic illustration of the intermolecular orientational correlation functions shown in Figure 8. (A) Typical preferred orientation of molecule 2 when located relative to the molecule 1 coordinate frame at $\theta_1 = 180°$ and $\phi_1 = 0°$. (B) Typical preferred orientation of molecule 2 when approaching molecule 1 along the x-axis i.e., $\theta_1 = 90°$ and $\phi_1 = 0°$. (C) Most likely orientation of molecule 2 when located above the central molecule along the z-axis with $\theta_1 = 0°$ and $\phi_1 = 0°$. The molecules in positions (A) and (C) are free to rotate around their central axis, running vertically in the plane of the page from (A) through the central molecule to (C).

the bottom left and right of the panel indicate that such an approach would favor interactions with a slightly canted T-like configuration where the oxygen atom and $C1M1_2$ group of the neighboring molecule would point toward the plane of the ring of the central molecule as illustrated in Figure 9B. The slightly positively charged $C1M1_2$ group is coordinated with the slightly negatively charged oxygen on the central molecule. As would be expected, this finding is consistent with the T-like configuration discussed for Panel (A) with electrostatic interactions. The smaller lobe below the origin of the coordinate reference axes shows that, though T-like configurations are seen to be generally favored it is also possible for THF molecules to interact via antiparallel face to face approach between molecular rings.

Panel (C) shows the preferred orientation of a molecule in the third region of the SDF shown in Figure 7, $\theta_1 = 0°$. Again the equatorial ring of intensity highlights the preference for perpendicular orientation of the interaction geometry between two tetrahydrofuran molecules, but in contrast to the wavelike form of the polar T-like molecular interaction, the smooth form of nonpolar interaction between two tetrahydrofuran molecules can be seen to be less orientationally sensitive to interactions with the CH_2 groups at the nonpolar end of the tetrahydrofuran molecule.

7. Void Structure

The results obtained by structure refinement of neutron scattering data are consistent with a liquid structure dominated by a T-like local arrangement of molecular rings. The efficiency of the resultant molecular packing can now be tested and the overall homogeneity of the liquid structure investigated. Recent simulation results[4] suggest the presence of cavities within the solvent structure. These cavities may enable the solvent to accommodate solvated electrons and hence may be an important structural reason for the solvent's intrinsic physicochemical properties.

To investigate the extent of void regions within the liquid, a search of the ≈29000 Å^3 volume of the refined model structure has been performed. Two searches identified respectively positions within the volume that are at least 1.25 Å or 1.5 Å from the surface of any atom in the system, calculated on a ∼0.3 Å spaced (x,y,z) grid that spanned the model. To define the atomic surfaces it was necessary to estimate the atomic radii. In this study the radii were taken from the Lennard-Jones parameters used to seed the structure refinement process and based on these criteria the results highlight the likely extent of finding cavities of at least 2.5 Å and 3.0 Å diameter within the liquid structure. Figure 10 shows the distribution of the two different sized cavities seen within a typical refined structural snapshot.

Figure 11 shows the surface chemistry of the void regions calculated by noting the type of atom closest to each point within a designated void. These histograms clearly show that voids form due to the poor packing of the largely nonpolar regions of the tetrahydrofuran molecule, as the dominant atomic species bounding the voids are the hydrogen atoms of the molecules' CH_2 groups. The surface chemistry of the larger 3.0 Å voids is completely dominated by C1, M1, and M2 atoms types while for the smaller 2.5 Å voids a small fraction (∼0.6%) of the surface is coordinated by the polar oxygen atom of the cyclic

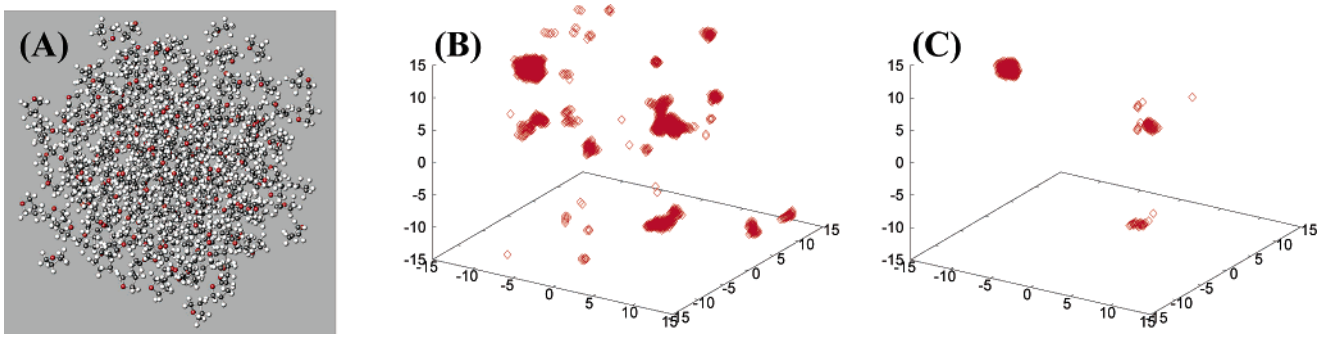

Figure 10. (A) Snapshot of the EPSR refined three-dimensional structure of liquid tetrahydrofuran. (B) Highlights void regions where the nearest atomic surface is greater than 1.25 Å from any point. (C) Highlights larger voids where the nearest atomic surface is greater than 1.5 Å distant.

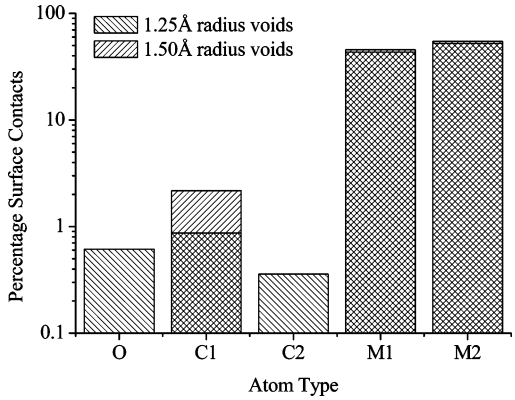

Figure 11. Void surface histogram for the structural snapshots shown in Figure 10. This graph shows the percentage of each atom type that bound the void-like regions within the liquid. Note the logarithmic ordinate scale.

ether ring. The ratio between M1 and M2 surface hydrogen sites bounding the void regions in all cases is close to 1. Noting that the M2 sites are electrically neutral and that there are no counterbalancing negatively polarized oxygen atom surface contributions, the electrostatic character of the void is likely to be slightly positive due to the slight positive polarization of the M1 hydrogen sites.

8. Conclusions

The results of this neutron scattering structural study confirm that voids appear to be an intrinsic component of the structure of pure tetrahydrofuran and that they appear to arise from the predominantly T-like packing of the molecules. In contrast to an earlier simulation study[4] this structural model, parametrized to neutron scattering data, suggests that the preferred radius of the void regions is of the order of 1.25 Å as opposed to 2.5 Å, and that a 1.5 Å radius void would be close to the maximum size likely to be found in the pure liquid. This difference appears to be due to the different definitions of the atomic radii used in the two studies, in particular this investigation is based upon an all-atom model of the molecular liquid, while the earlier work[4] was based upon a five-point unified atom model for tetrahydrofuran. Additionally the earlier study[4] used distance to atomic centers and not distance to atomic surfaces as the void search criterion. Once allowance is made for these different approaches, the two studies fall into reasonable agreement. Our finding of a slightly positive electrostatic character for the void volumes supports the idea that these regions would favor the solvation of negatively charged electrons in agreement with the known characteristics of this liquid.

The intermolecular electrostatic interactions involving the oxygen sites and slightly polarized CH_2 units appear to structure the orientational interactions between tetrahydrofuran molecules when these are mediated by the more polar end of the molecule. In contrast the interactions at the nonpolar end of the molecule appear to be relatively orientationally unhindered though driven by the general molecular packing within the liquid to conform to the T-like structural interaction motif.

Acknowledgment. We thank the Engineering and Physical Sciences Research Council for funding under Grant GR/K/12465 and the Council for the Central Laboratory of the Research Councils for access to their neutron facility: ISIS, Rutherford Appleton Laboratory, Oxfordshire, U.K.

JA0583057